

Electronic Supplementary Information

High-performance flexible strain sensors based on silver film wrinkles modulated by liquid PDMS substrates

Yifan Xu,^a Miaogen Chen,^{*a} Senjiang Yu,^{*b} and Hong Zhou^a

^a Key Laboratory of Intelligent Manufacturing Quality Big Data Tracing and Analysis of Zhejiang Province, College of Science, China Jiliang University, Hangzhou 310018, P.R. China

^b Key Laboratory of Novel Materials for Sensor of Zhejiang Province, College of Materials and Environmental Engineering, Hangzhou Dianzi University, Hangzhou 310018, P.R. China

* Corresponding authors:

phycmg@cjl.u.edu.cn (M. Chen);

sjyu@hdu.edu.cn (S. Yu)

Supplementary Figures and captions

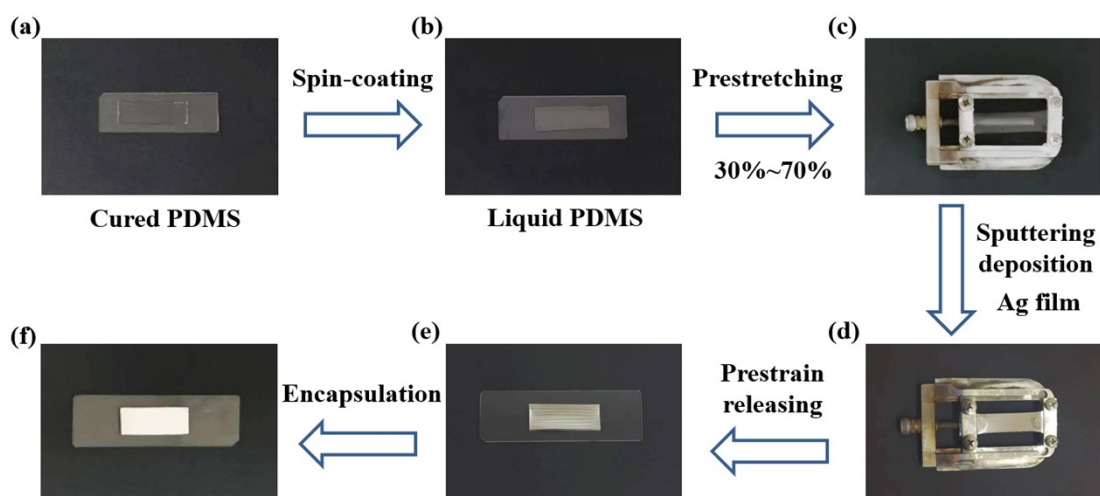


Figure S1. Photographs of the sample during the preparation process. The experimental procedure can be divided into six steps: preparation of a solidified PDMS sheet (a), spin-coating a liquid PDMS thin layer (b), uniaxial stretching (c), silver film deposition (d), prestrain releasing (e), and device encapsulation (f).

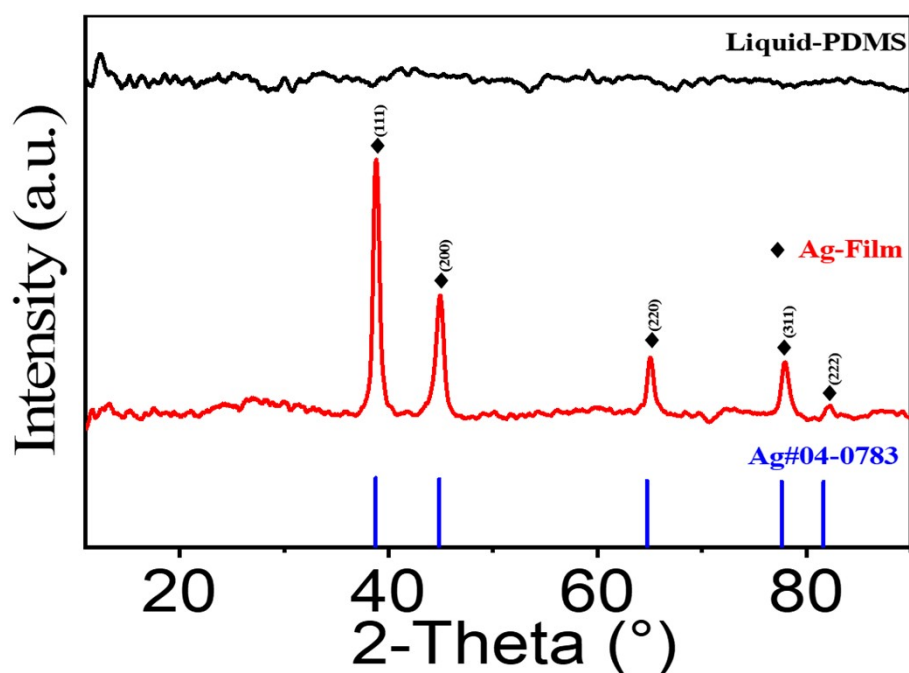


Figure S2. X-ray diffraction (XRD) patterns of the Ag film on liquid PDMS and the pure liquid PDMS substrate. The Ag diffraction peaks can be seen clearly.

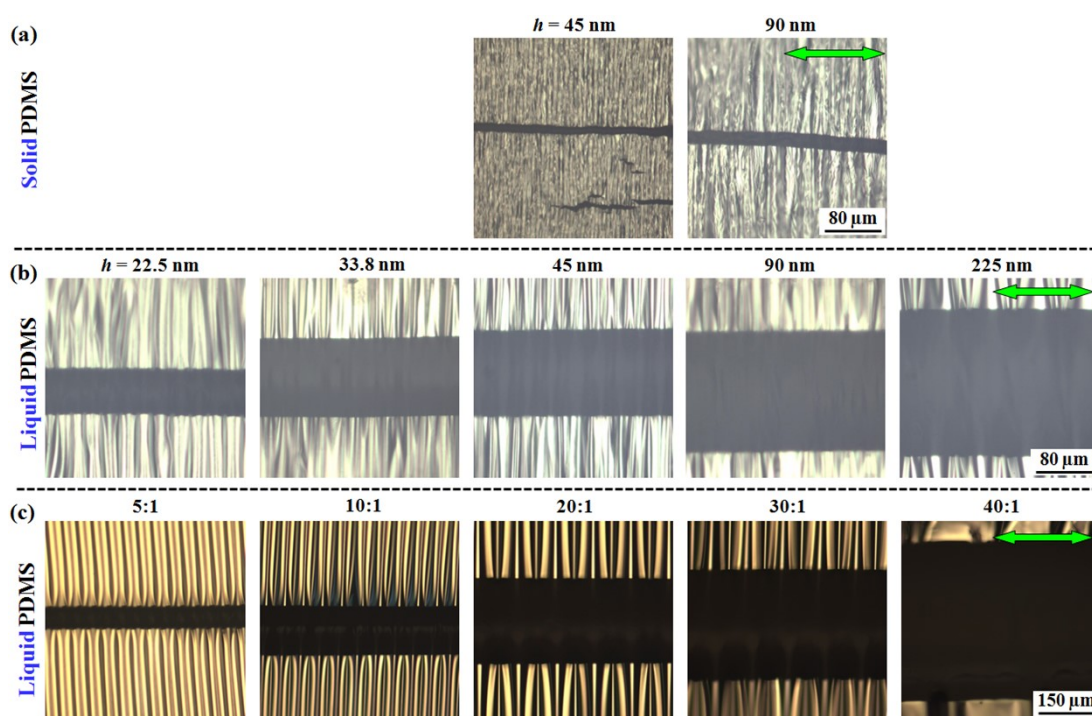


Figure S3. (a) Crack morphologies of silver films with different thicknesses on the solid PDMS substrates (20:1). (b) Crack morphologies of silver films with different thicknesses on the liquid PDMS substrates (20:1). (c) Crack morphologies of silver films with $h = 90$ nm on the liquid PDMS substrates with different prepolymer-to-crosslinker ratios. The bidirectional arrows present the prestrain loading direction. The image sizes are $280 \times 280 \mu\text{m}^2$ for (a,b) and $520 \times 520 \mu\text{m}^2$ for (c).

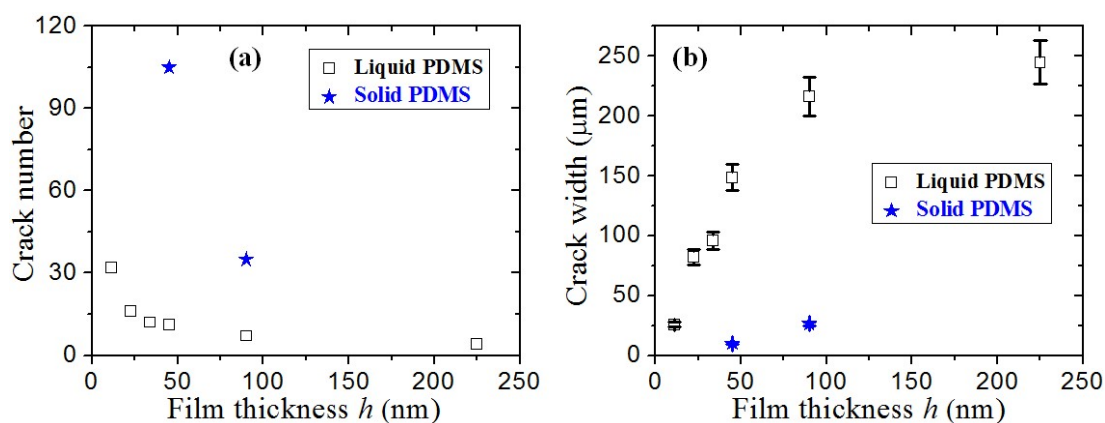


Figure S4. Dependences of crack number (a) and crack width (b) on the film thickness for silver films deposited on the liquid and solid PDMS substrates.

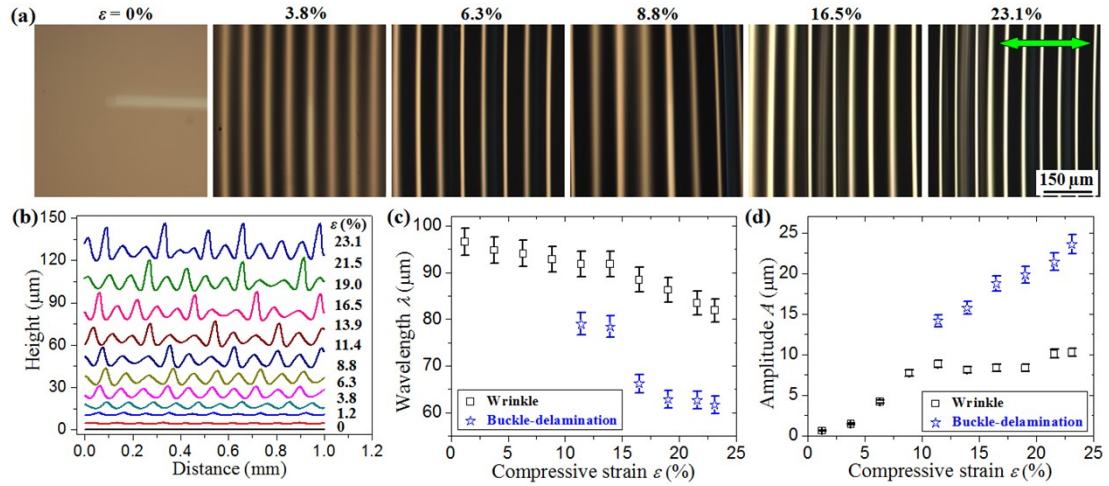


Figure S5. (a) In situ morphological evolution of the silver film with $h = 225$ nm on the liquid PDMS substrate with prepolymer-to-crosslinker ratio of 20:1 during prestrain releasing. The data above the images represent the compressive strain. Each image has a size of $538 \times 538 \mu\text{m}^2$. (b) Surface profiles under different compressive strains. (c,d) Evolutions of wavelength λ (c) and amplitude A (d) of both wrinkles and buckle delaminations with the compressive strain ε . Note that the wrinkles first form for small strains and then buckle delaminations appear. The wrinkles and buckle delaminations are coexisted in the final stage.

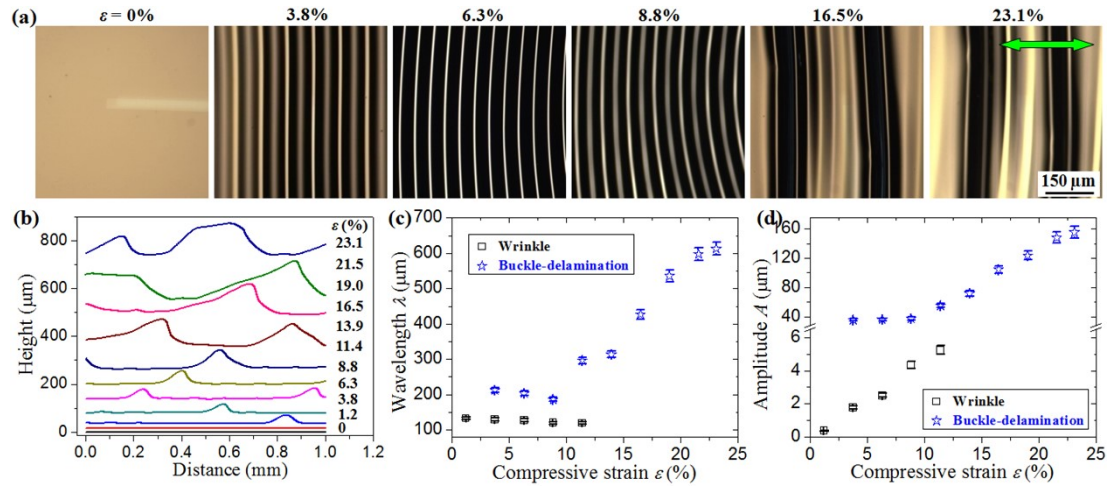


Figure S6. (a) In situ morphological evolution of the silver film with $h = 360$ nm on the liquid PDMS substrate with prepolymer-to-crosslinker ratio of 20:1 during prestrain releasing. Each image has a size of $538 \times 538 \mu\text{m}^2$. (b) Surface profiles under different compressive strains. (c,d) Evolutions of wavelength λ (c) and amplitude A (d) of both wrinkles and buckle delaminations with the compressive strain ε . Note that the buckle delaminations are dominant and the wrinkles are almost disappeared for larger compressive strains.

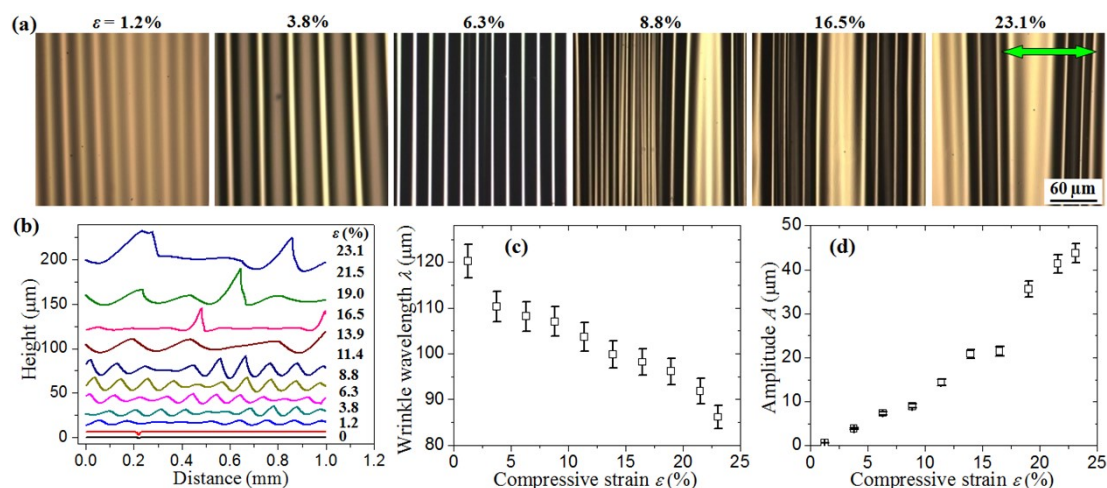


Figure S7. (a) In situ morphological evolution of the silver film with $h = 90$ nm on the liquid PDMS substrate with prepolymer-to-crosslinker ratio of 40:1 during prestrain releasing. Each image has a size of $220 \times 220 \mu\text{m}^2$. (b) Surface profiles under different compressive strains. (c,d) Evolutions of wavelength λ (c) and amplitude A (d) of wrinkles or ridges with the compressive strain ε . Note that the wrinkles first form for small strains and then ridges appear. The ridges are dominant and the wrinkles are almost disappeared for larger compressive strains.

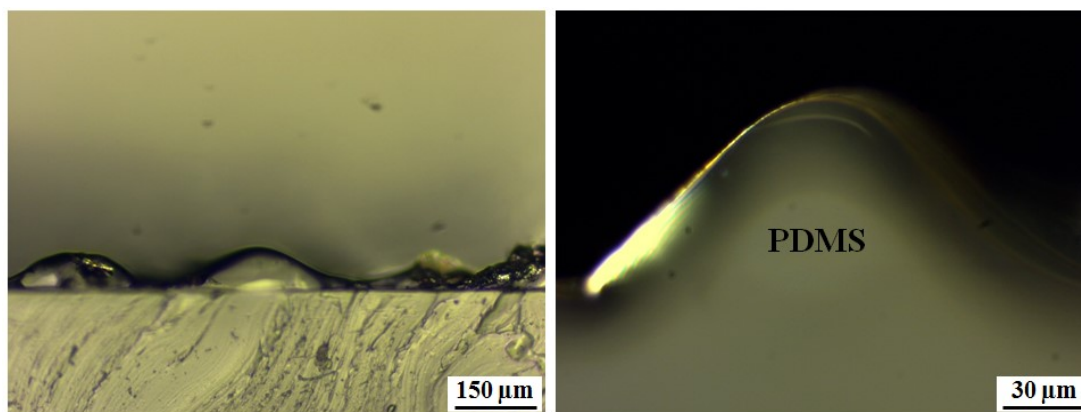


Figure S8. Cross-sectional profiles of the ridge structures in the silver film ($h = 90$ nm) on the liquid PDMS substrate with prepolymer-to-crosslinker ratio of 40:1. It is clear that the PDMS is conformably deformed with the silver film and no interfacial delamination is observed.

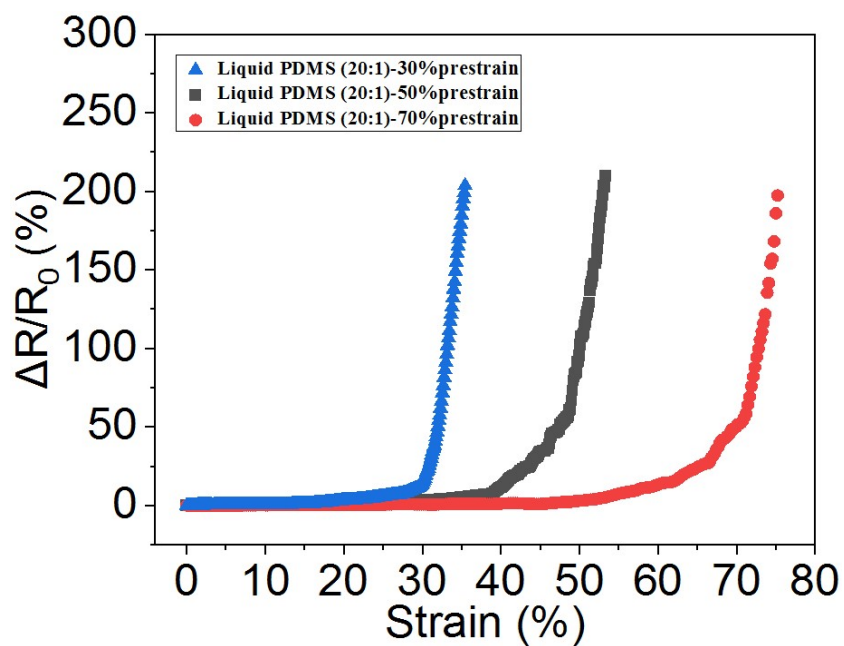


Figure S9. Relative electrical resistance variation under strain loading for the Ag films ($h = 90$ nm) on the liquid PDMS substrates (20:1) for different prestrains (30% and 50%).

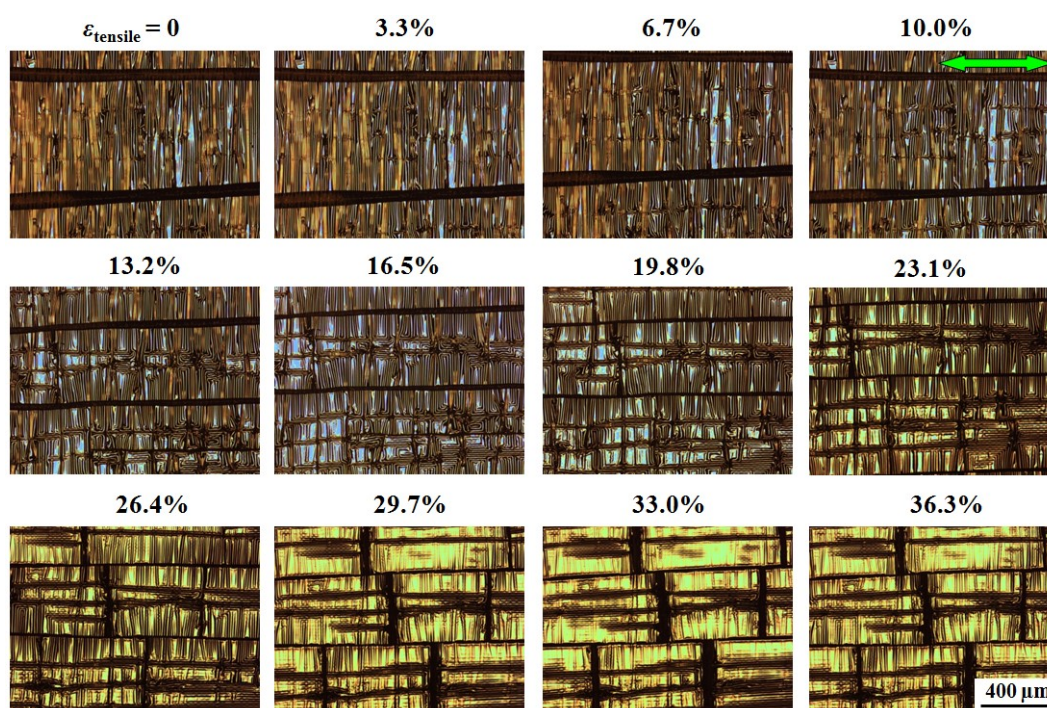


Figure S10. (a) Evolution of surface morphologies under strain loading for the Ag film ($h = 90$ nm) on the liquid PDMS substrate (20:1) prepared by 30% prestrain. Each image has a size of $1390 \times 1043 \mu\text{m}^2$.

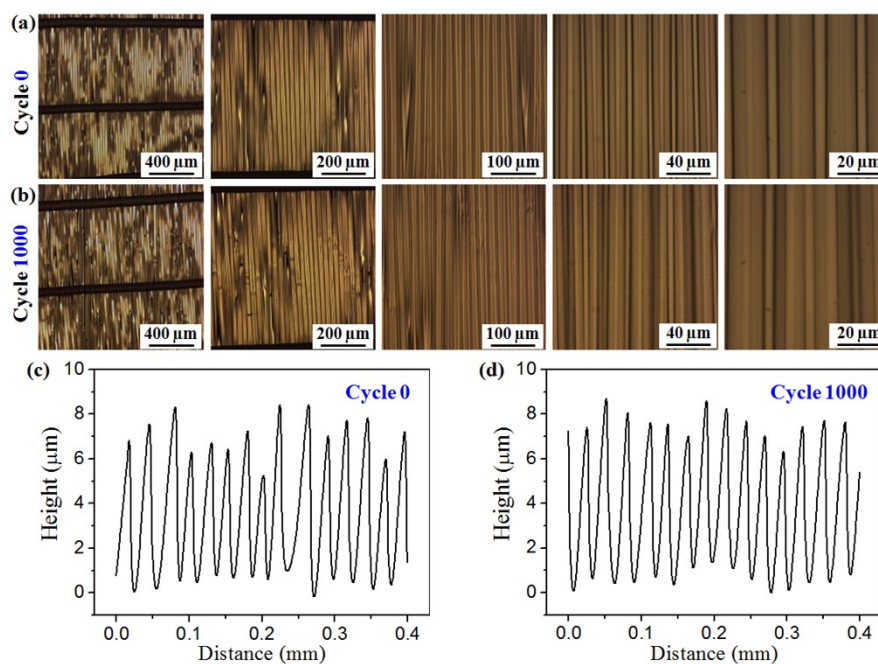


Figure S11. (a,b) Comparison of the surface morphologies of the silver film ($h = 90$ nm) on the liquid PDMS substrate (10:1) before (just after the prestrain releasing, namely as cycle 0) and after 1000 cycles at 10% mechanical strain. (c,d) Comparison of the profiles before and after 1000 cycles at 10% strain. No obvious variation of the morphologies and profiles during the cycling process can be observed.

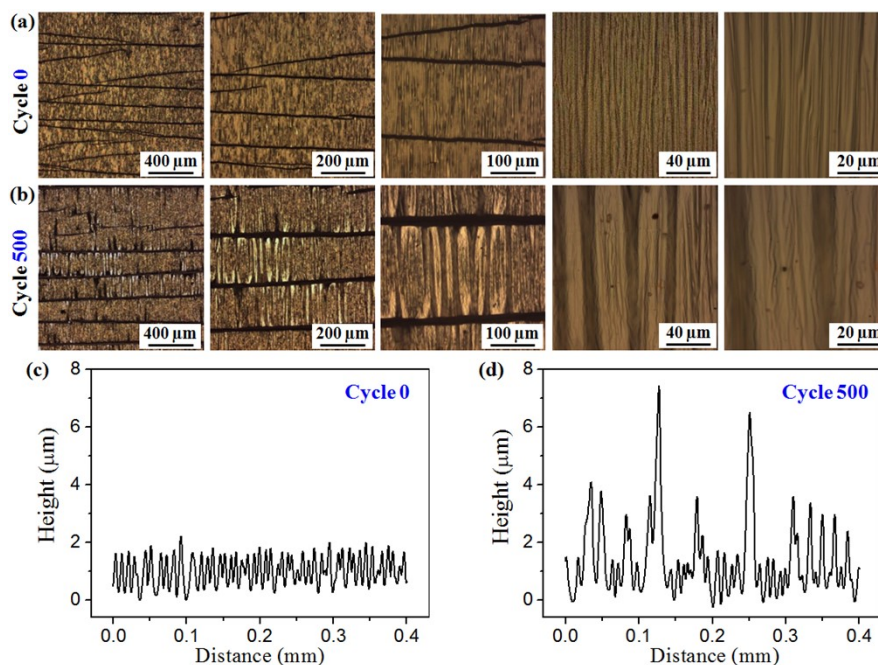


Figure S12. (a,b) Comparison of the surface morphologies of the silver film (90 nm) on the Solid PDMS substrate (10:1) before and after 500 cycles at 10% mechanical strain. (c,d) Comparison of the profiles before and after 1000 cycles at 10% strain. It is clear that interfacial delaminations occur during the cycling process, leading to the obvious variation of the morphologies and profiles.

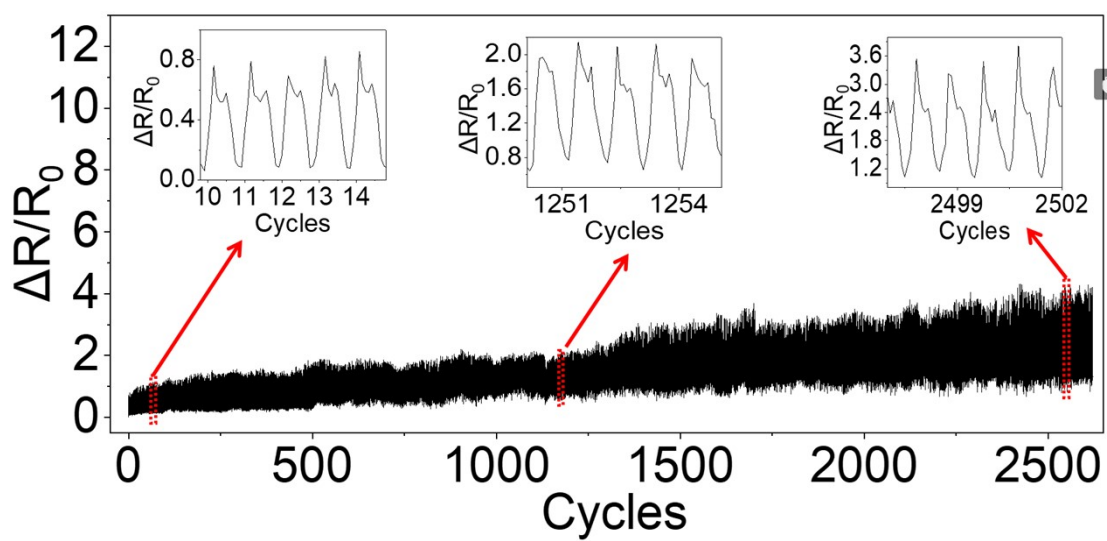


Figure S13. Durability of the strain sensor based on the silver film/solid PDMS system ($h = 90$ nm, prepolymer-to-crosslinker ratio 20:1, and prestrain 30%) under more than 2500 cycles at 5% strain.